Expanded View Figures

Figure EV1. Characterization of *EML1* patient- and *EML1*-heKO-derived iPS cells.

A Immunocytochemical analyses of iPS cells reveal that cells stain positive for the pluripotency-associated markers Tra1-60, Tra-1-81, and SSEA3. Following 4 weeks of *in vitro* differentiation and immunocytochemical analyses, derivatives of all three germ layers such as ß-III-tubulin+ (ß-III-Tub, ectoderm), alpha-1-fetoprotein+ (AFP, endoderm), and smooth muscle actin+ cells (SMA, mesoderm) could be detected.

B High-resolution SNP karyotyping reveals integrity of the karyotype. Note: (A) and (B) depict representative data of *EML1* patient 1–derived iPS cells. (C), *EML1* patient 1 and *EML1* patient 2 (D)-specific mutations were confirmed by sequencing.

C *EML1* patient 1 and *EML1* patient 2.

D Specific mutations were confirmed by sequencing.

E Genetic validation of selected *EML1*-heKO clones. PCR primers are designed to recognize the *EML1* wild-type allele or the integration of the puromycin cassette. Note: Detection of the integration of the puromycin cassette simultaneously to detection of WT allele indicates heterozygous *EML1*-heKO.

F qRT–PCR shows reduced expression levels of *EML1* in *EML1*-heKO-derived iPS cells confirming the heterozygous *EML1*-heKO. Three biological replicates, data in graphs are represented as means ± SD. Significance based on two-way ANOVA and Tukey's multiple-comparison test, ***$P = 0.0001$.

Data information: For statistical analyses, see the source data for this figure. Scale bars, (A) 100 μm, SMA and AFP 25 μm.
Source data are available online for this figure.

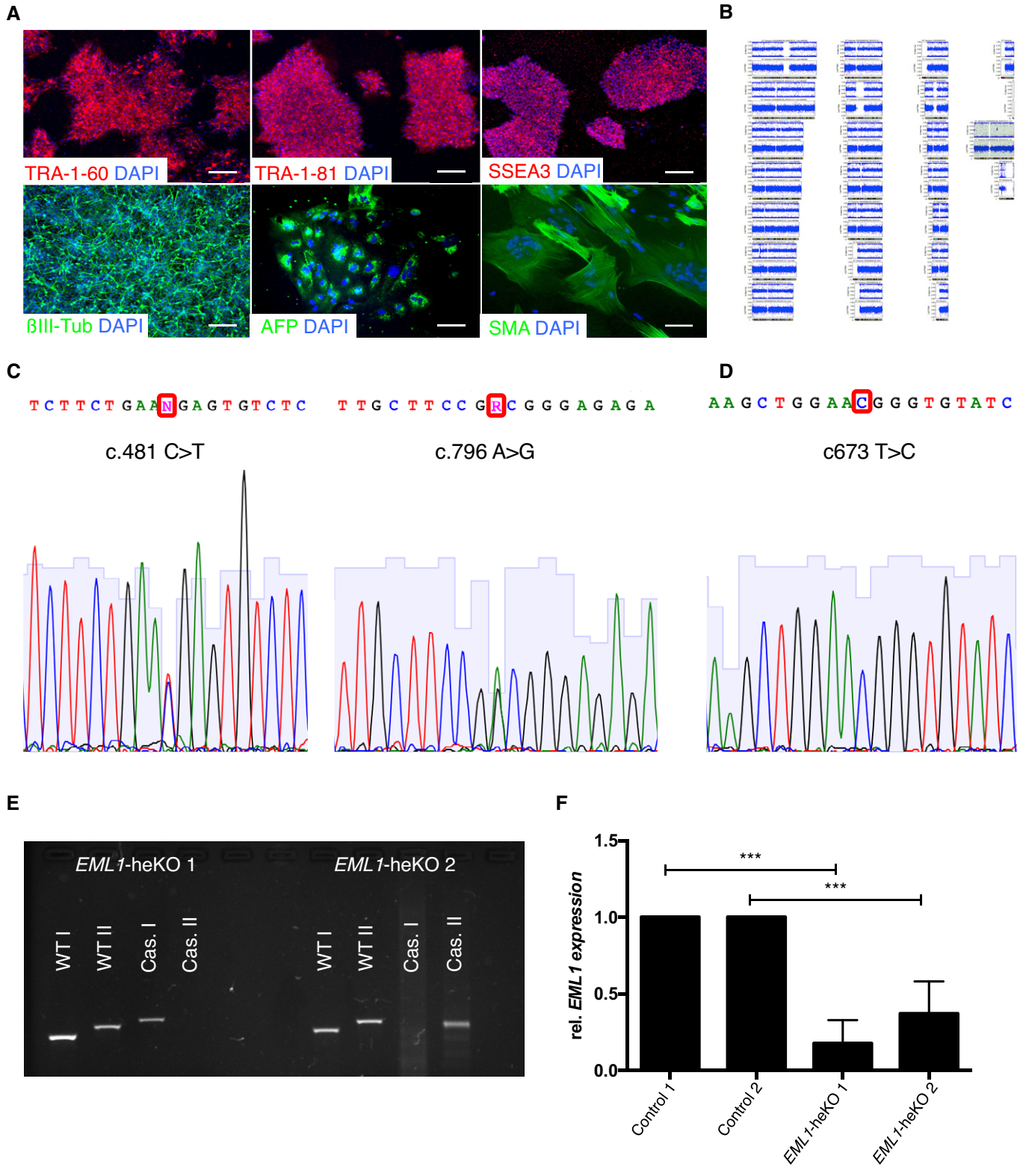
A
TRA-1-60 DAPI
TRA-1-81 DAPI
SSEA3 DAPI
βIII-Tub DAPI
AFP DAPI
SMA DAPI
B
C
T C T T C T G A A N G A G T G T C T C
T T G C T T C C G R C G G G A G A G A
c.481 C>T
c.796 A>G
D
A A G C T G G A A C G G G T G T A T C
c673 T>C
E
EML1-heKO 1
EML1-heKO 2
WT I
WT II
Cas. I
Cas. II
WT I
WT II
Cas. I
Cas. II
F
rel. EML1 expression
1.5
1.0
0.5
0.0
***
***
Control 1
Control 2
EML1-heKO 1
EML1-heKO 2

Figure EV1.

Figure EV2. RG cell division mode and EpoD-mediated tubulin stabilization.

A Immunocytochemical analyses of day 20 ± 2 control- and *EML1*-deficient cerebral organoids stained for p-Vim (mitotic cells) and TPX2 (labeling the mitotic spindle). Dotted lines indicate the VZ surface and RG-cell division mode, squares indicate areas enlarged below.

B PAX6-positive cortical progenitors derived from control, *EML1*-heKO, and *EML1*-heKO treated with EpoD exhibit ARL13B-positive primary cilia.

C Immunoblot for acetylated tubulin in control and *EML1*-deficient cortical progenitors under control- (−) or EpoD-treated (+) condition.

D Quantification of relative protein signal intensities of the immunoblot shown in C based on n = 3 biological replicates of independent experiments. Signals were normalized to actin.

Data information: Bar graphs show mean with SEM, significance based on two-way ANOVA with Bonferroni's multiple-comparison test, $^{**}P = 0.0047$. For individual *P*-values, see the source data for this figure. Scale bars: (A) 50 μm, enlarged 10 μm; (B) 5 μm.

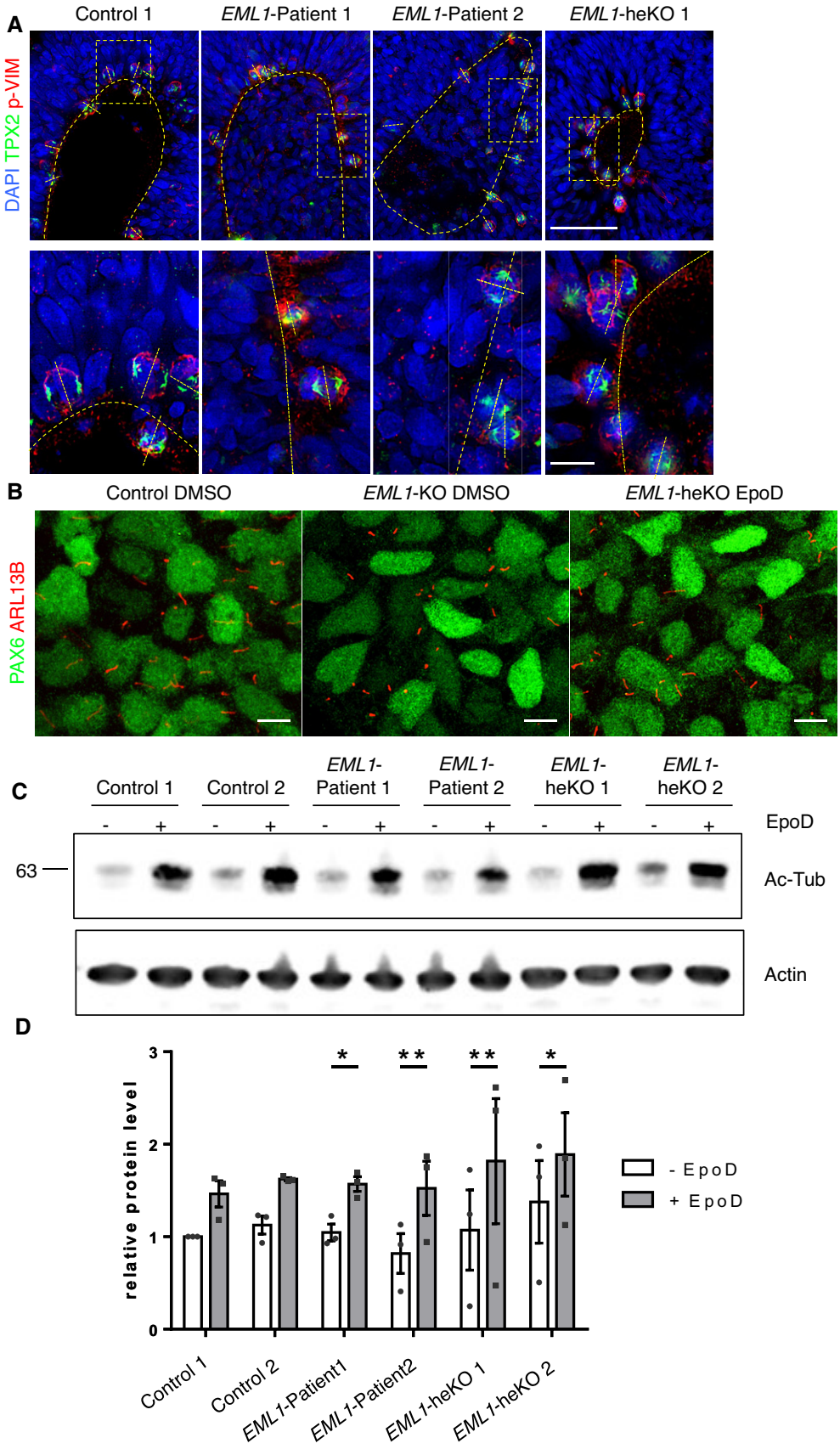
A
Control 1
EML1-Patient 1
EML1-Patient 2
EML1-heKO 1
DAPI TPX2 p-VIM
B
Control DMSO
EML1-KO DMSO
EML1-heKO EpoD
PAX6 ARL13B
C
Control 1
Control 2
EML1-Patient 1
EML1-Patient 2
EML1-heKO 1
EML1-heKO 2
EpoD
63
Ac-Tub
Actin
D
relative protein level
- EpoD
+ EpoD
Control 1
Control 2
EML1-Patient1
EML1-Patient2
EML1-heKO 1
EML1-heKO 2

Figure EV2.

Figure EV3. Overview of scRNAseq experiment, *EML1* expression, and further characterization of RG to bRG cells.

A Schematic of scRNA-seq experiment procedure. VZ areas from nine control and nine *EML1*-heKO-derived organoids from three independent batches were dissected and pooled. Image was designed using biorender.com.

B Dotplot of known marker gene expression in control-derived cells. Scaled average normalized expression for the respective gene in each cell type is indicated by a continuous color scale. Number of cells in the respective cluster expressing the genes is represented by the size of the dots.

C Normalized expression of *EML1* in day 33 ± 2 control-derived cerebral organoid cells per cell type investigated by scRNAseq (three pooled batches and three organoids each).

D Heatmap of z-scaled gene expression of extracellular matrix (ECM) and basal radial glial (bRG) genes in the RG to bRG cell cluster derived from either control or *EML1*-heKO organoids.

E Overview of a day 33 ± 2 cortical structure derived from control or *EML1*-heKO stained for the pan-neuronal marker MAPT, counterstained with DAPI. The VZ is encircled; the heterotopic region is highlighted by a dotted line and labeled with #.

F COL1A2, MEIS2, and MAPT magnification for control and *EML1*-heKO, counterstained with DAPI. The VZ is encircled; The heterotopic region is highlighted by a dotted line and labeled with #.

Data information: Scale bars: (E and F) 50 μm.
Source data are available online for this figure.

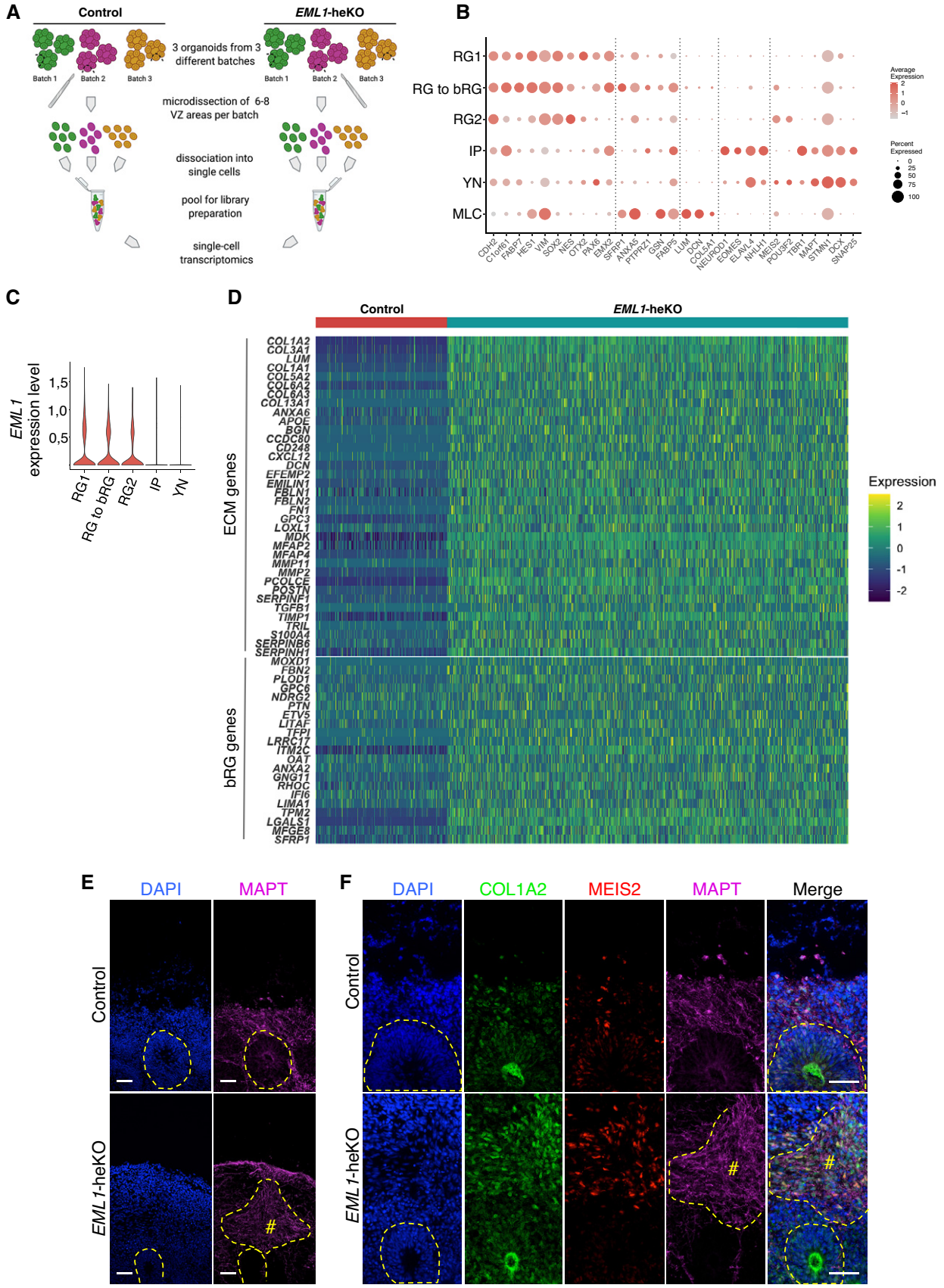
A
Control
EML1-heKO
Batch 1
Batch 2
Batch 3
3 organoids from 3 different batches
microdissection of 6-8 VZ areas per batch
dissociation into single cells
pool for library preparation
single-cell transcriptomics
B
RG1
RG to bRG
RG2
IP
YN
MLC
Average Expression
Percent Expressed
C
EML1 expression level
1,5
1,0
0,5
RG1
RG to bRG
RG2
IP
YN
D
Control
EML1-heKO
ECM genes
bRG genes
Expression
E
DAPI
MAPT
Control
EML1-heKO
F
DAPI
COL1A2
MEIS2
MAPT
Merge
Control
EML1-heKO

Figure EV3.

Figure EV4. Ectopic progenitor cell proliferation in *EML1*-deficient organoids and Fluvastatin-mediated YAP inhibition.

A Immunocytochemical analyses of control and *EML1*-deficient organoids (day 20 ± 2) for phosphorylated vimentin (p-VIM) counterstained with DAPI. Note: Dividing p-Vim-positive cells located at the apical surface of VZ areas in control organoids. *EML1* patients- and *Eml1*-heKO-derived organoids reveal ectopically localized p-VIM-positive cells outside VZ areas. Apical surface of VZ areas highlighted by dotted line and p-VIM-positive cells outside the VZ areas indicated with arrowheads.

B Quantification of mitotic cells located at the apical side of VZ areas in control and *EML1*-deficient conditions (three batches, three organoids each, significance based on Kruskal–Wallis test and Dunn's *post hoc* test, $P = 0.0001$; for detailed statistical information, see the source data for this figure).

C Immunocytochemical analyses of control and *EML1*-deficient organoids (day 20 ± 2) for BrdU and Ki67 counterstained with DAPI.

D Normalized expression of *YAP1*, *CCND3*, *CDK6*, and *CYR61* in all cell types. Split violins show expression in control and *EML1*-heKO (three pooled batches and three organoids each). Asterisks indicate Bonferroni corrected *P*-values (Wilcoxon rank sum test: ***< 0.001, **< 0.01, *< 0.05, ns, not significant; for detailed statistical information, see the source data for this figure).

E Immunocytochemical analyses of p-VIM and YAP1 in *EML1*-heKO-derived organoids in DMSO- or Fluvastatin-treated condition. Squares indicate areas enlarged in adjacent parts of the panel.

F Immunocytochemical analyses of NCAD in *EML1*-heKO-derived organoids in DMSO- or Fluvastatin-treated condition counterstained with DAPI.

Data information: Scale bars: (A, C, E, and F) 50 μm, (E) enlarged 10 μm.
Source data are available online for this figure.

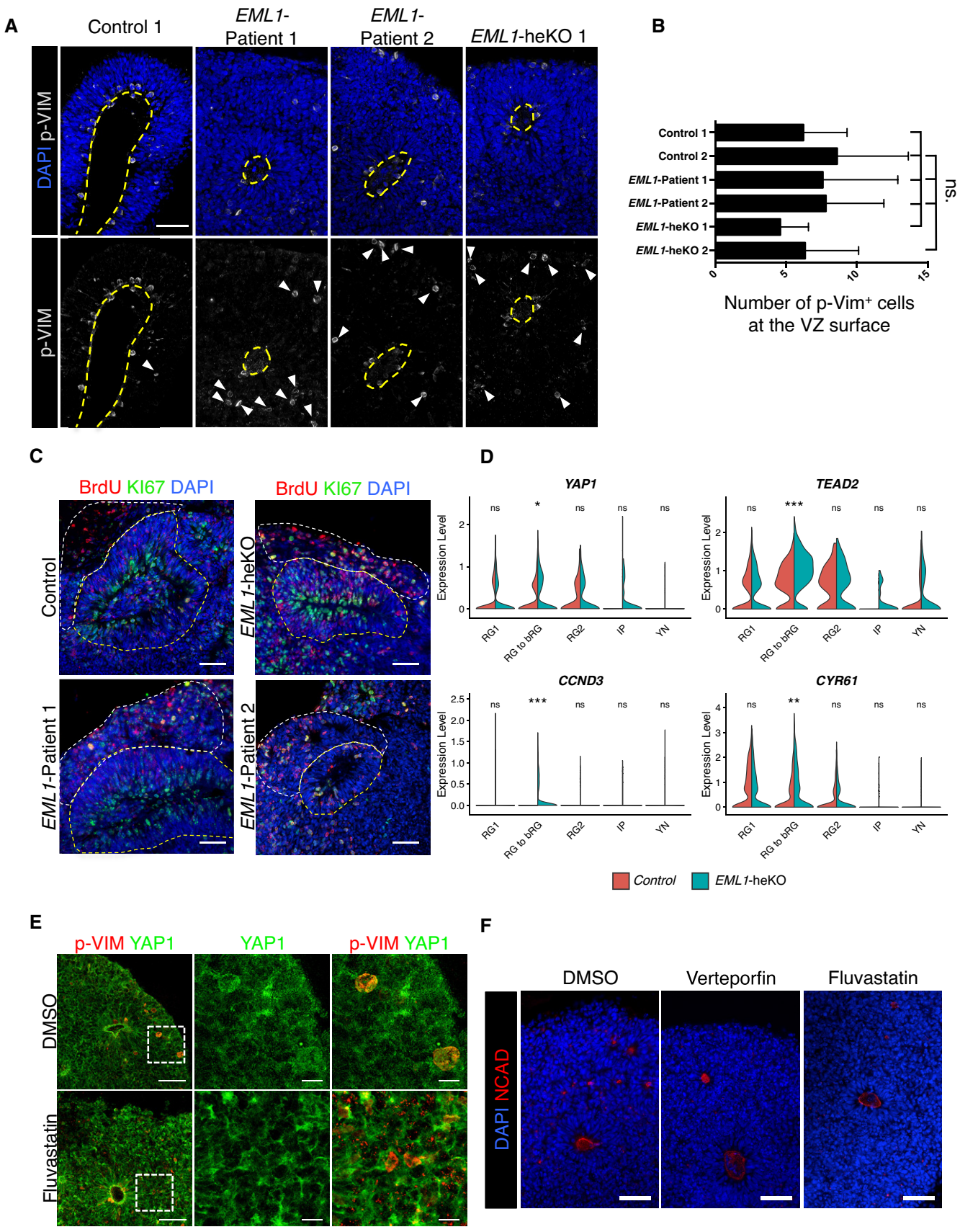
A
Control 1
EML1-Patient 1
EML1-Patient 2
EML1-heKO 1
DAPI p-VIM
p-VIM
B
Control 1
Control 2
EML1-Patient 1
EML1-Patient 2
EML1-heKO 1
EML1-heKO 2
ns.
0
5
10
15
Number of p-Vim+ cells at the VZ surface
C
BrdU KI67 DAPI
BrdU KI67 DAPI
Control
EML1-heKO
EML1-Patient 1
EML1-Patient 2
D
YAP1
TEAD2
CCND3
CYR61
Expression Level
RG1
RG to bRG
RG2
IP
YN
Control
EML1-heKO
E
p-VIM YAP1
YAP1
p-VIM YAP1
DMSO
Fluvastatin
F
DMSO
Verteporfin
Fluvastatin
DAPI NCAD

Figure EV4.